What neutron stars tell about the hadron–quark phase transition: a Bayesian study

Based on Tekatsy et al. 2023 (https://arxiv.org/abs/2303.00013)

Problem: dense matter EoS

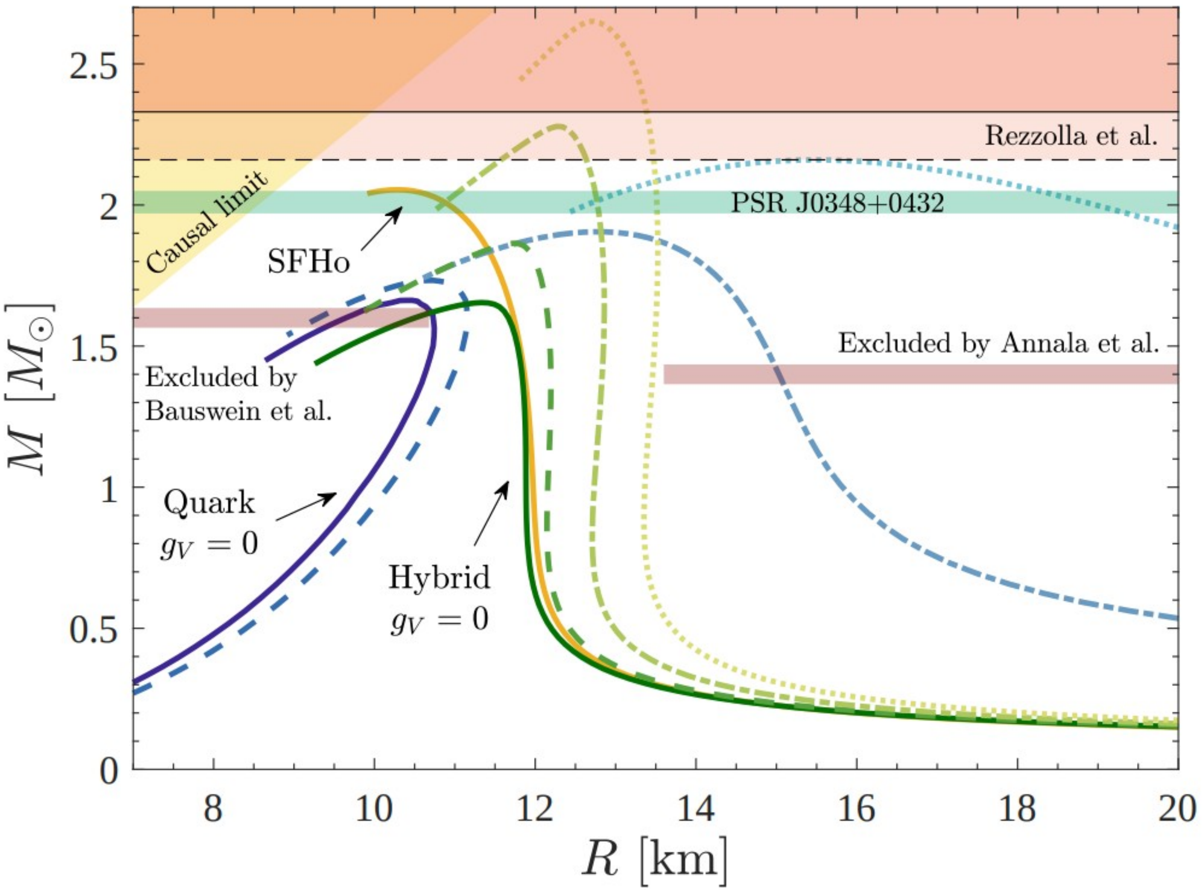

Phase transition to quark matter

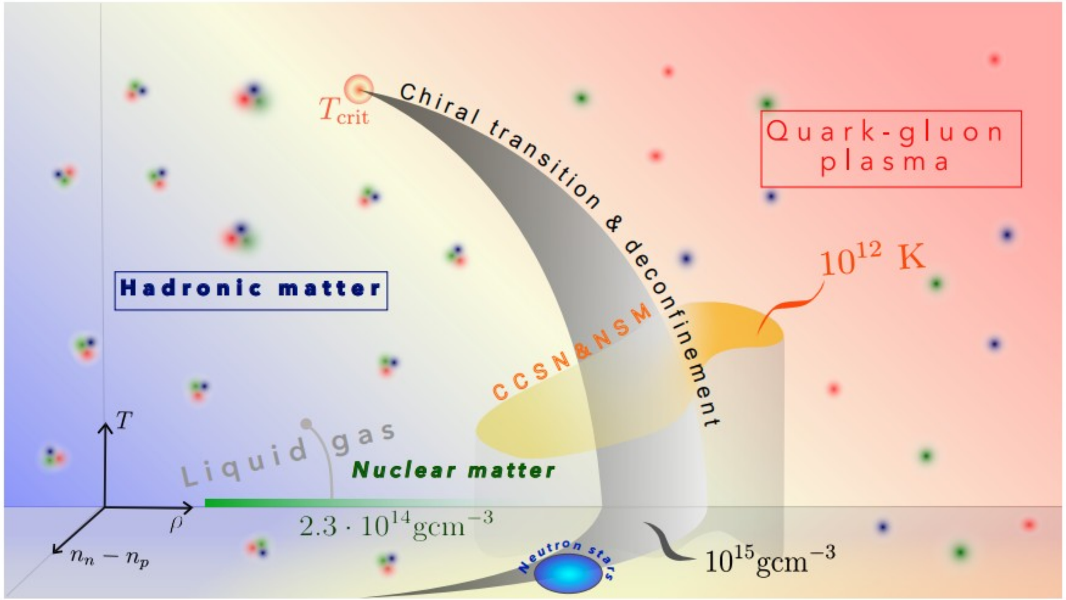

Figure 1. Illustrative QCD phase diagram. The *x*-, *y*-, and *z*-axis represent density, temperature and isospin asymmetry density $n_n - n_p$. The regime of late post-bounce phase of core-collapse supernovae and of neutron-star mergers are indicated by the orange band and grey shade.

Jakobus et al. (2022)

EoS parameters

- Hadronic EoS: fixed to SFHo or DD2
- 2 parameters for phase transition
- 2 parameters for quark model

Priors / minimal constraints

- pQCD calculations
- There is always a hadronic part (low density)

Mass constraints (pulsars)

$$p(M_{\max}|\boldsymbol{\vartheta}) \propto \prod_{i=1,2} \frac{1}{2}\left[1 + \operatorname{erf}\left(\frac{M_{\max}(\boldsymbol{\vartheta}) - M_i}{\sqrt{2}\sigma_i}\right)\right]$$

$$\times \frac{1}{2}\left[1 - \operatorname{erf}\left(\frac{M_{\max}(\boldsymbol{\vartheta}) - M_U}{\sqrt{2}\sigma_U}\right)\right]$$

Mass constraints

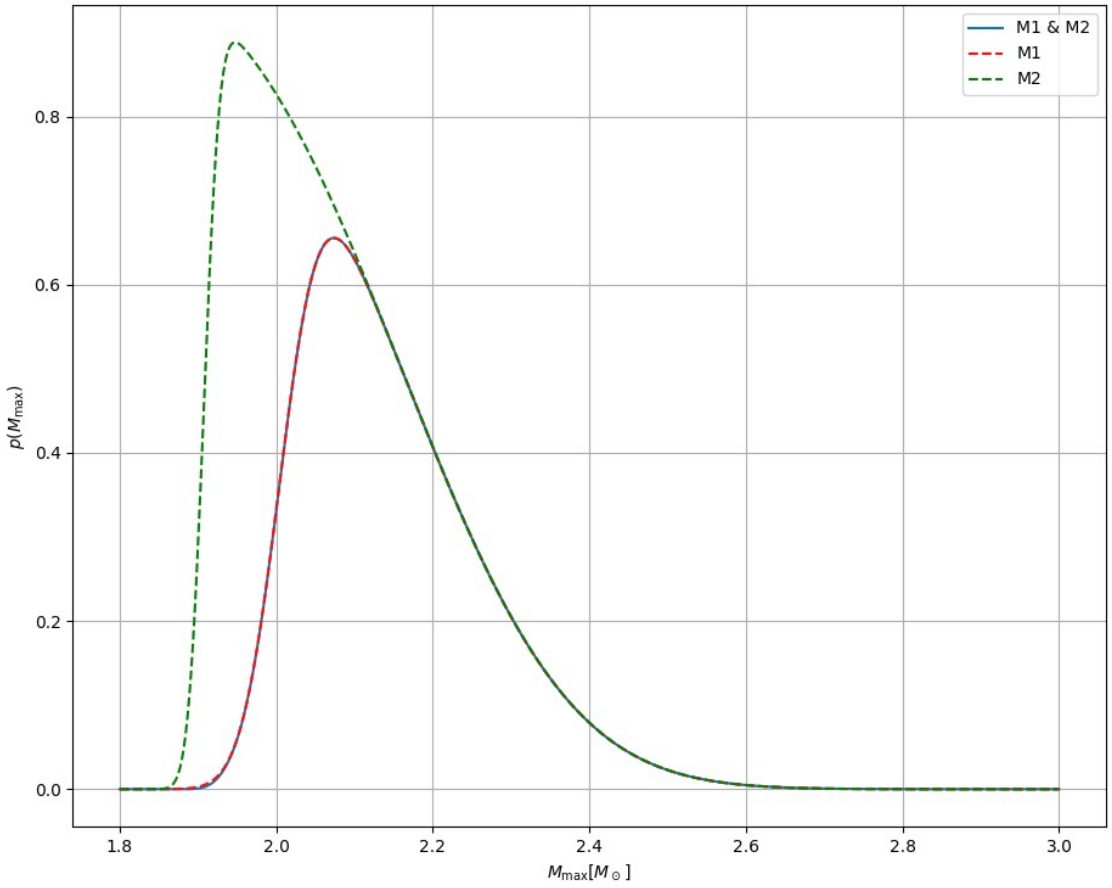

$$M_1 = 2.01 \pm 0.04$$
$$M_2 = 1.908 \pm 0.016$$
$$M_U = 2.16 \pm 0.17$$

$$M_{PSRJ\,0740+6620} = 2.08 \pm 0.07$$

R-M measurements (NICER)

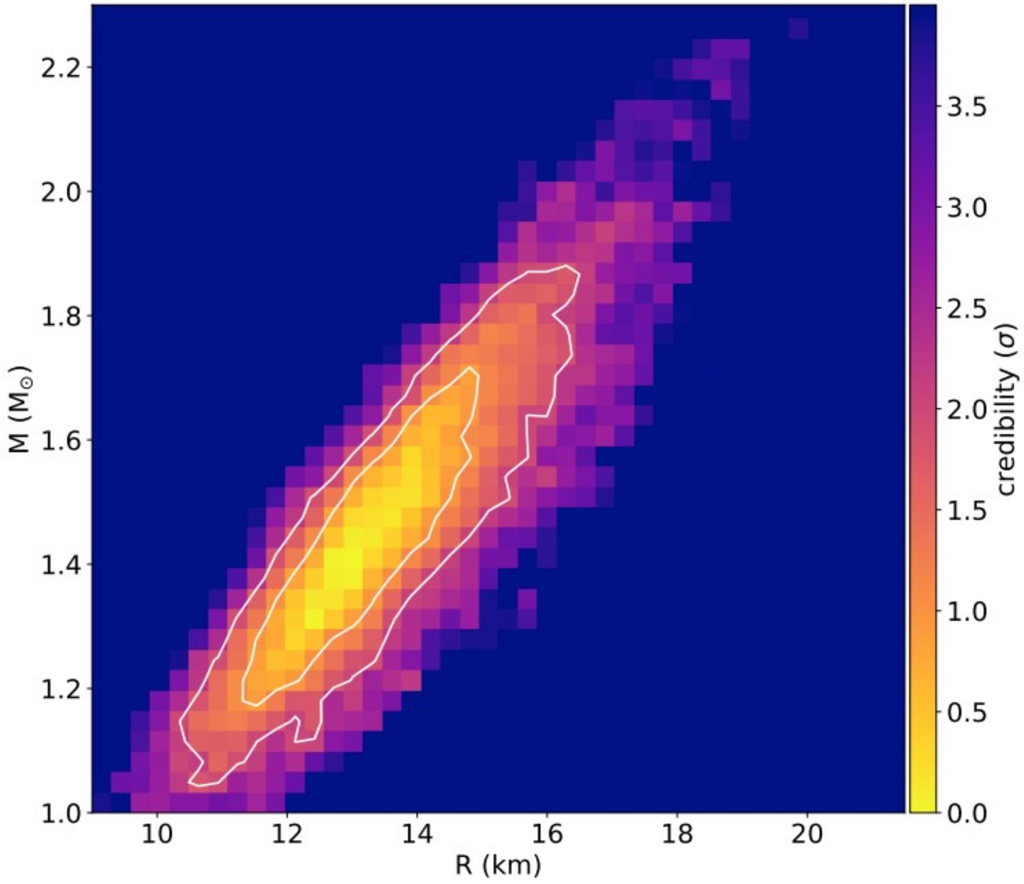

PSR J0030+0451
PSR J0740+6620

NICER measurements

$$
\begin{aligned}
p(\mathrm{NICER}|\boldsymbol{\vartheta}) &\propto \int \mathrm{d}M \mathrm{d}R \, p_{\mathrm{N}}(M,R)\delta(R - R(M,\boldsymbol{\vartheta})) \\
&= \int \mathrm{d}M \, p_{\mathrm{N}}(M, R = R(M,\boldsymbol{\vartheta}))\,. \qquad (17)
\end{aligned}
$$

Tidal deformability of GW170817

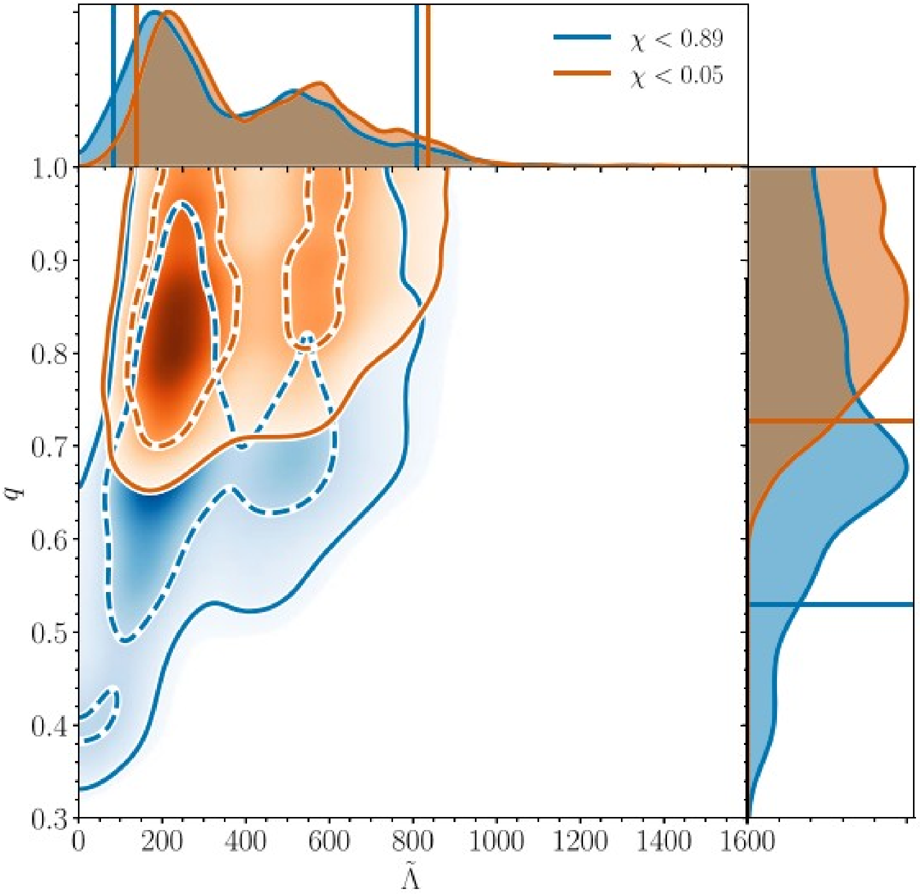

FIG. 12. PDFs for the tidal parameter $\tilde{\Lambda}$ and mass ratio q using the PhenomPNRT model for the high-spin (blue) and low-spin (orange) priors. Unlike Fig. 11, the posterior is not reweighted by the prior, so the support that is seen at $\tilde{\Lambda} = 0$ is due to smoothing from the kernel density estimator (KDE) that approximates the distribution from the discrete samples. The 50% (dashed lines) and 90% (solid lines) credible regions are shown for the joint posterior. The 90% credible interval for $\tilde{\Lambda}$ is shown by vertical lines, and the 90% lower limit for q is shown by horizontal lines.

LIGO Collaboration and Virgo Collaboration (2019)

Tidal deformability of GW170817

$$p(\tilde{\Lambda}|\boldsymbol{\vartheta}) \propto \int_{M_{\rm eq}}^{M_{\rm max}} \mathrm{d}M_1 \, p_{\rm GW}(\tilde{\Lambda}(M_1, \mathcal{M}, \boldsymbol{\vartheta}), q(M_1, \mathcal{M})) \,, \tag{19}$$

Additional constraints

- GW170817: was it a black hole? Hypermassive NS hypothesis.
- GW190814: Mass gap object?
- HESS measurements

Putting it all together

- Consistency with pQCD + lower mass limit
- NICER measurements
- Tidal deformability
- Additional scenarios

$$p(\mathrm{data}|\boldsymbol{\vartheta}) = p(M_{\mathrm{max}}|\boldsymbol{\vartheta})\, p(\mathrm{NICER}|\boldsymbol{\vartheta})\, p(\tilde{\Lambda}|\boldsymbol{\vartheta})$$

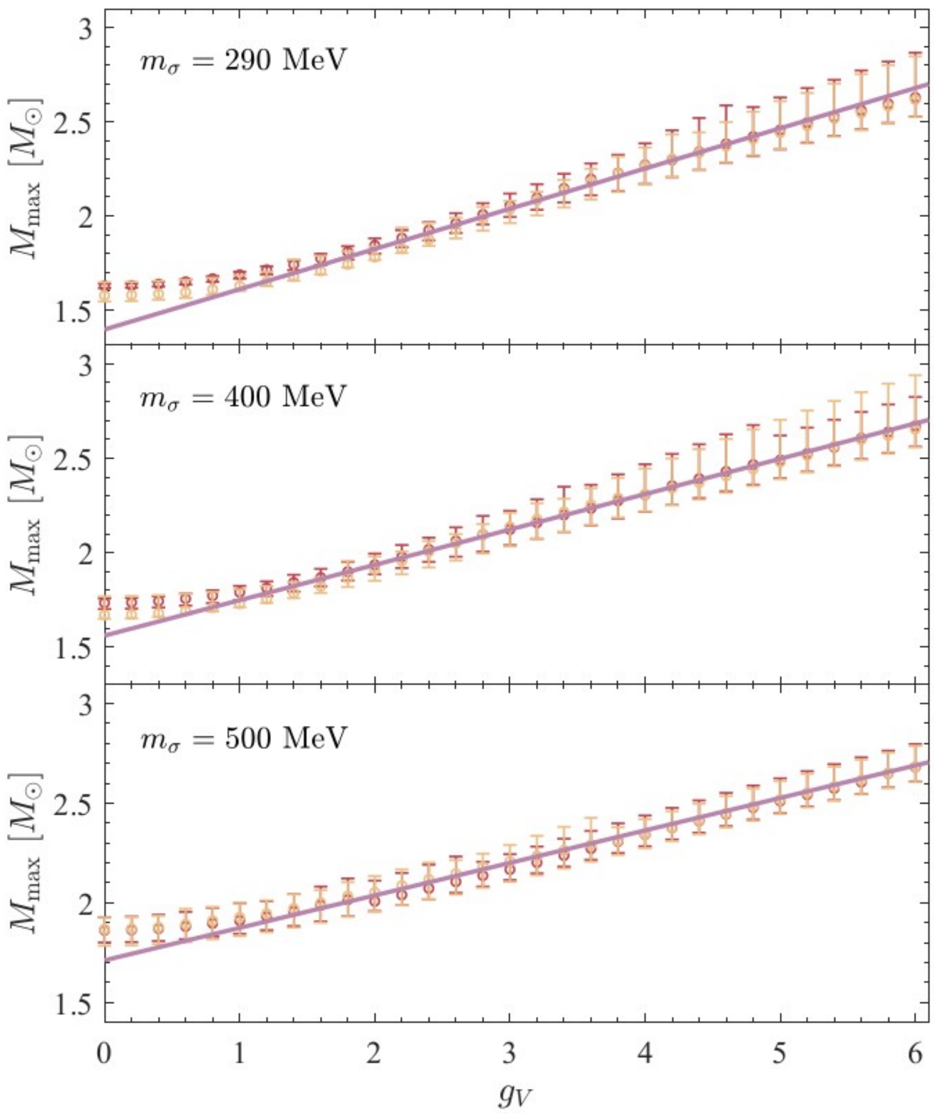

- gv-Mmax relation is almost linear

Results of Bayesian analysis

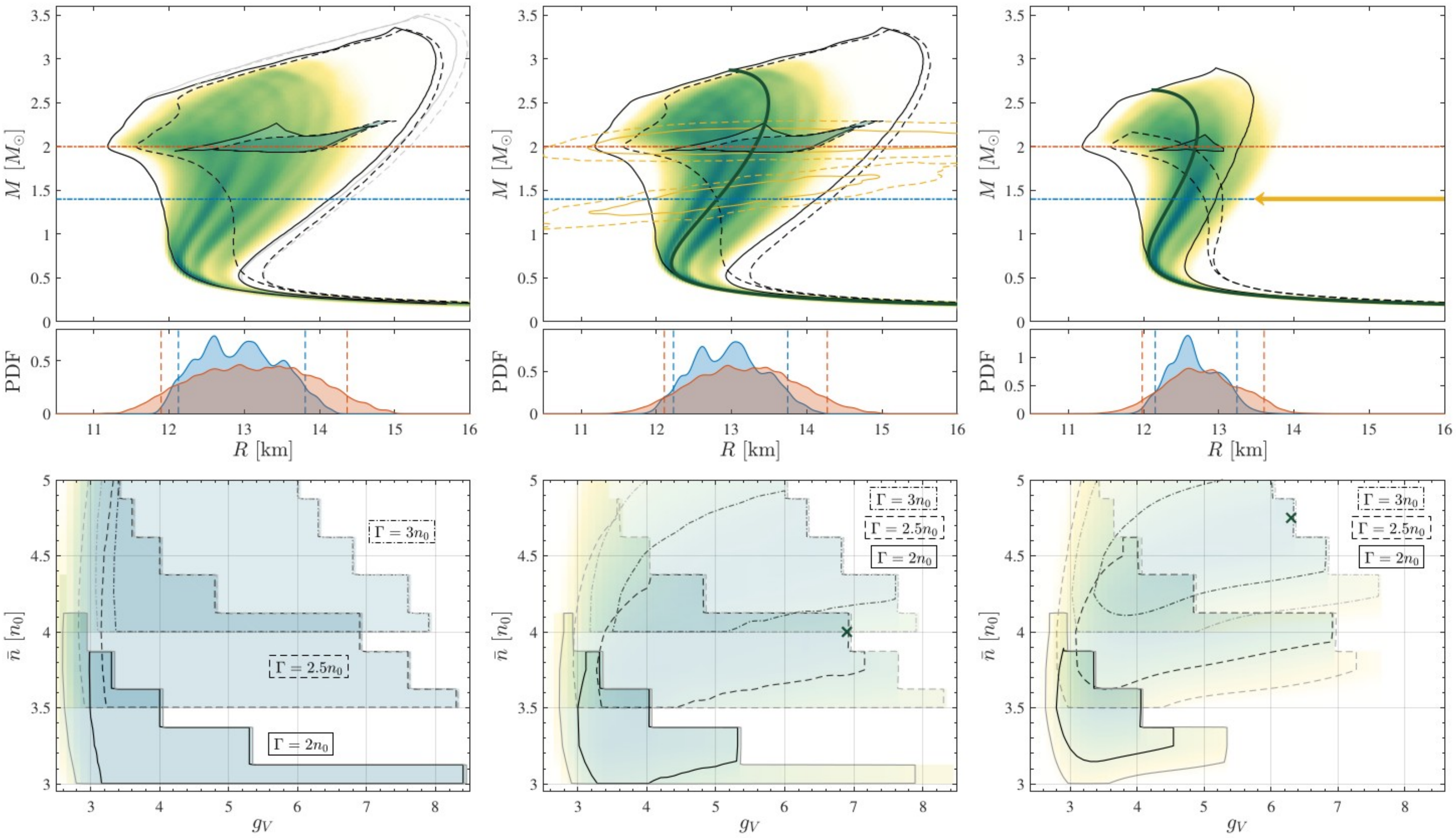

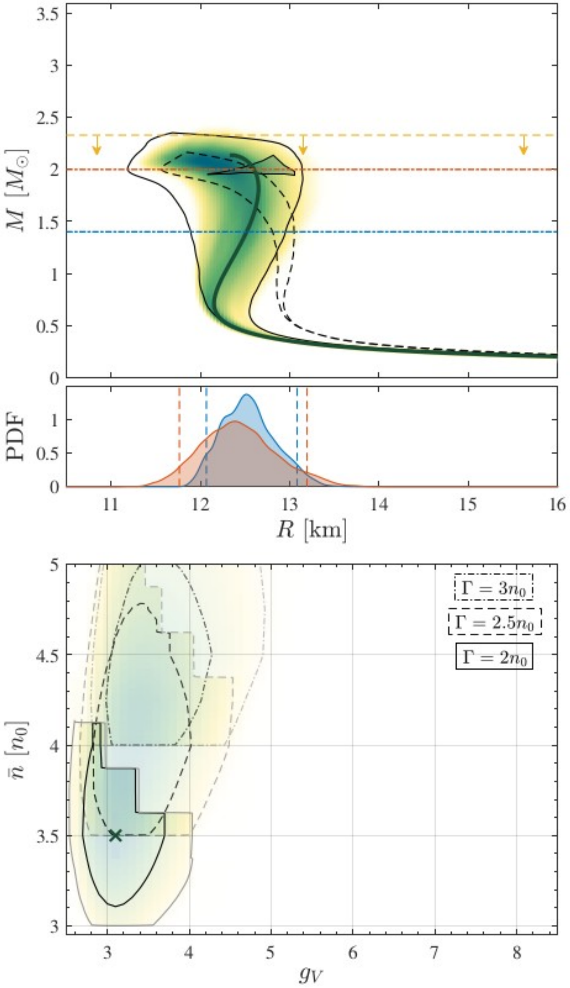

FIG. 4. Same as in Fig. 2 but with the upper mass constraint from the hypermassive NS hypothesis also applied, in addition to the NICER and GW170817 measurements.

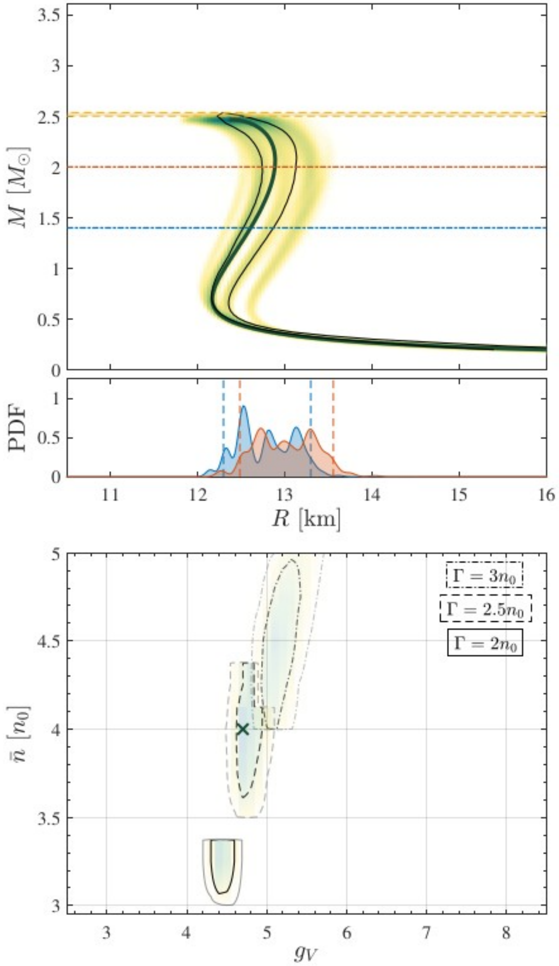

FIG. 5. Same as in Fig. 4 but instead of taking into account the upper mass bound based on the hypermassive NS hypothesis we only include the constraint from the BH hypothesis, while identifying the mass-gap object in GW190814 as a NS.

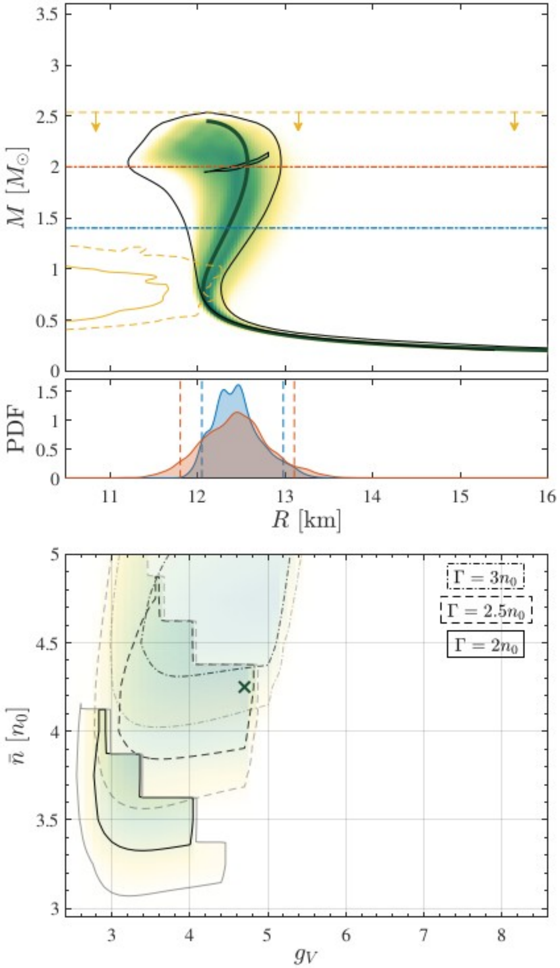

FIG. 8. Same as in Fig. 2 but with the constraint from the central compact object inside HESS J1731-347 also applied, in addition to the NICER and tidal deformability measurements, and the BH hypothesis.

Properties of quark cores

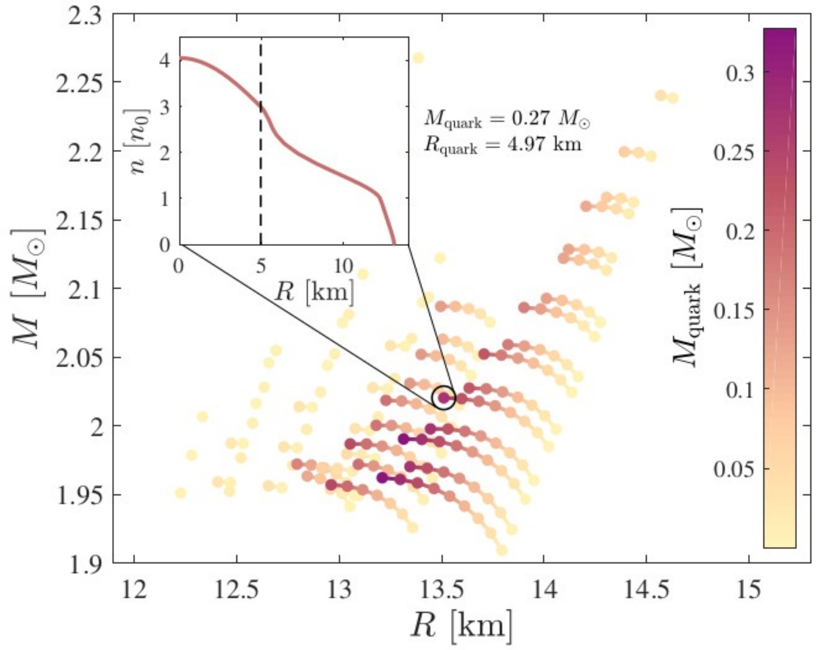

FIG. 3. Masses of quark cores for hybrid stars that develop such a core. The inset shows the radial dependence of the baryon density inside one of the hybrid stars that have a sizeable quark core. The vertical dashed line represents the boundary between the quark core and the outer layers.

Phase transition properties

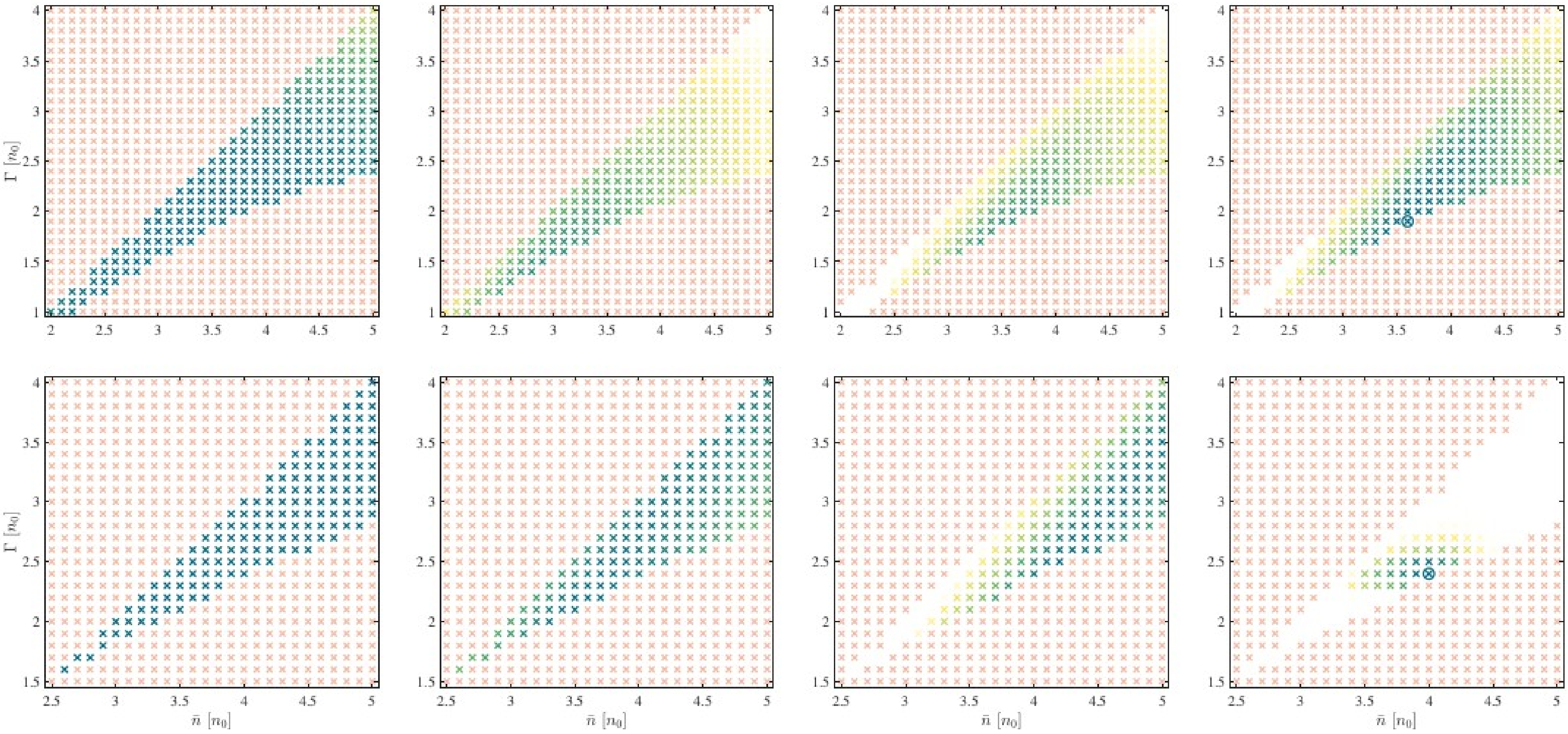

Summary

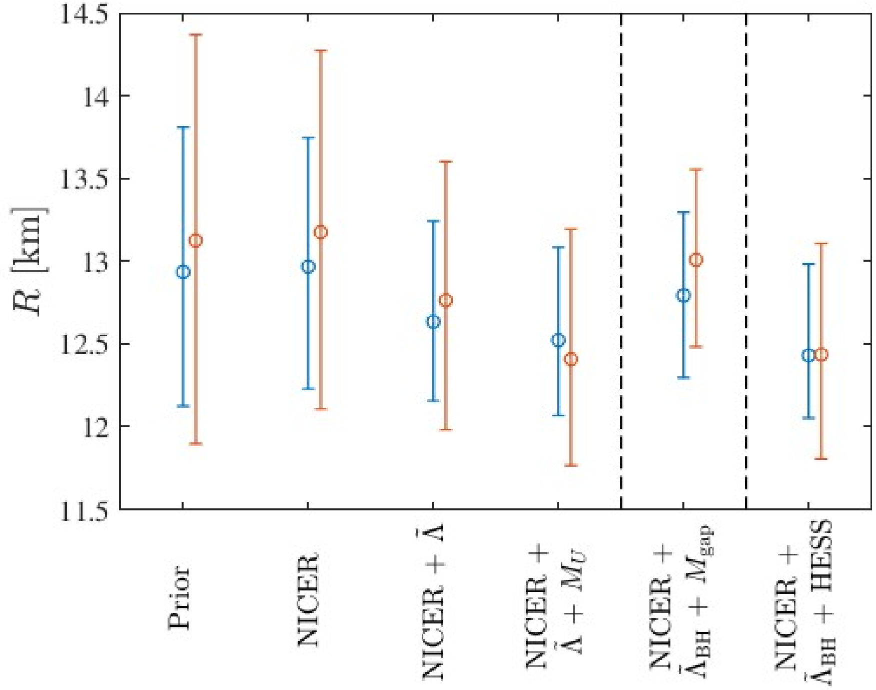

TABLE I. Median values of radii for 1.4 $M_\odot$ and 2 $M_\odot$ NSs for the different astrophysical constraints investigated in this paper. The errors represent the 90% credible intervals. All values correspond to NSs with hadronic EoSs given by the SFHo model.

Measurement	$R_{1.4}$ [km]	$R_{2.0}$ [km]
Prior (pQCD + $2M_\odot$)	$12.93^{+0.88}_{-0.81}$	$13.12^{+1.24}_{-1.23}$
NICER	$12.97^{+0.78}_{-0.74}$	$13.18^{+1.10}_{-1.07}$
NICER + $\tilde{\Lambda}$	$12.63^{+0.61}_{-0.48}$	$12.76^{+0.84}_{-0.78}$
NICER + $\tilde{\Lambda}$ + M_U	$12.52^{+0.56}_{-0.46}$	$12.41^{+0.79}_{-0.64}$
NICER + $\tilde{\Lambda}_{BH}$ + M_{gap}	$12.79^{+0.50}_{-0.50}$	$13.01^{+0.55}_{-0.53}$
NICER + $\tilde{\Lambda}_{BH}$ + HESS	$12.43^{+0.55}_{-0.38}$	$12.44^{+0.67}_{-0.63}$

Conclusions

- Astrophysical constraints can constrain the hadron-quark transition
-